Journal of Network Intelligence
Taiwan Ubiquitous Information
 ISSN 2414-8105 (Online)
Volume **10**, Number **4**, November **2025**

Food digestion algorithm: A novel optimization algorithm

Shu-Chuan Chu

Information Engineering College
Guangzhou City Construction College, Guangzhou 510925, China

School of Artificial Intelligence
Nanjing University of Information Science and Technology, Nanjing 210044, China
scchu0803@sdust.edu.cn

Zhi-Yuan Shao

College of Computer Science and Engineering
Shandong University of Science and Technology, Qingdao 266590, China
504853328@qq.com

Jeng-Shyang Pan*

School of Artificial Intelligence
Nanjing University of Information Science and Technology, Nanjing 210044, China

Department of Information Management
Chaoyang University of Technology, Taichung 41349, Taiwan
jspan@ieee.org

*Corresponding author: Jeng-Shyang Pan

Received March 31, 2025, revised July 16, 2025, accepted September 16, 2025.

Abstract. *This paper proposes a novel meta-heuristic algorithm inspired by the process of food digestion in the human body. We have named this algorithm the Food Digestion Algorithm (FDA). Food is digested at three different sites, which is used to simulate particle updating at these sites. The update of particles in each respective site not only depends on their own state, but is also affected by the state of particles in the previous digestion site. This correlation speeds up the process of particle optimization search and makes it easier to jump out of the local optimal solution. We tested the proposed algorithm using the CEC2013 test set and compared its performance with six classical algorithms. The results indicate that for 28 functions, the FDA demonstrated superior convergence performance compared to the Genetic Algorithm (GA) and the Sine Cosine Algorithm (SCA). It also outperformed the Particle Swarm Optimization (PSO), Differential Evolution (DE), Cat Swarm Optimization (CSO), and the Auqila Algorithm (AO) on most functions. Furthermore, the FDA exhibited greater stability than the other algorithms.*
Keywords: Food digestion algorithm; Meta-heuristic algorithm; Swarm intelligence; CEC2013.

1. **Introduction.** Since the birth of meta-heuristic algorithms, they have solved many real-life problems for people. They have made significant contributions to various fields, such as image processing [1–4], power generation prediction [5] , UAV [6, 7], vehicle routing planning [8], stock prediction [9], wireless sensor networks [10–12], ontology matching [13, 14], health-care [15, 16], among others. There are two main characteristics of

meta-heuristic algorithms. One is exploration, and the other is exploitation. By balancing exploration and exploitation, the meta-heuristic algorithm can escape from local optima and thus obtain a good search result [17, 18]. Different meta-heuristic algorithms have different optimization capabilities. As the No Free Lunch (NFL) theorem [19] states, no single algorithm can solve problems across all domains; hence, new meta-heuristic algorithms are constantly emerging. Meta-heuristic algorithms can be categorized by various criteria. In this paper, they are divided into four categories. The first category is swarm intelligence, which includes Particle Swarm Optimization (PSO) [20], Grey Wolf Optimizer (GWO) [21], Aquila Optimizer (AO) [22], Whale Optimization Algorithm (WOA) [23], Cat Swarm Optimization (CSO) [24], Gannet Optimization Algorithm (GOA) [25], and others. The second category is evolutionary algorithms, which includes Genetic Algorithm (GA) [26], Differential Evolution (DE) [27], and others. The third category is human-based algorithms, which includes the Imperialist Competitive Algorithm (ICA) [28], and others. The fourth category is physics-based algorithms, which include Equilibrium Optimizer (EO) [29], Gravitational Search Algorithm (GSA) [30], Sine Cosine Algorithm (SCA) [31], and others.

Inspired by the digestion process of food in the human body, we propose a new meta-heuristic algorithm. There are three main sites for food digestion in the human body: the oral cavity, the stomach, and the small intestine. Food undergoes physical and chemical digestion here [32]. In the oral cavity, the process of physical digestion involves mastication by the teeth and agitation by the tongue. In contrast, chemical digestion mainly involves the digestion of starch by salivary amylase [33]. In the stomach, the process of physical digestion of food is mainly achieved through peristalsis, contraction, and diastole of the stomach. In contrast, the process of chemical digestion of food is primarily the digestion of proteins by pepsin [34–36]. In the small intestine, peristalsis impacts the physical digestion process of food, while various digestive enzymes drive the chemical digestion process [37, 38]. In this paper, we model the particle update process by simulating both the physical and chemical digestion processes of food in these three sites. When we compared six classical algorithms with FDA on the CEC2013 test set, the experimental results showed that FDA has strong performance.

In this paper, Section 2 describes the inspiration for the Food Digestion Algorithm (FDA) and its modeling process. Section 3 compares and analyzes the test results. Section 4 gives the conclusion.

2. **Food Digestion Algorithm.**

Each meta-heuristic algorithm may be suitable for solving specific real-world problems; therefore, the development of new meta-heuristic algorithms is crucial for addressing real-world challenges in emerging domains. This section introduces a novel meta-heuristic algorithm, the Food Digestion Algorithm, detailing its inspiration and modeling process. To enhance the readability of the paper, a notation table is provided to explain the terms used.

2.1. **Source of Inspiration.**

There are three main sites for food digestion in the human body: the oral cavity, stomach, and small intestine, as shown in the Figure 1. Food digestion in all three sites involves two processes: physical digestion and chemical digestion [32]. Both processes break down food from large molecules into small molecules; the key distinction lies in the fact that physical digestion applies mechanical force to food, whereas chemical digestion employs digestive enzymes to break it down.

In the oral cavity, physical digestion mainly involves the mechanical breakdown of food through chewing by the teeth and movement by the tongue, while chemical digestion primarily consists of starch breakdown by salivary amylase [39]. Early in chewing, the

TABLE 1. Notation table

Notation	Instruction
$Food_i^t$	It denotes the i-th particle of the t-th generation.
$Food_i^{t+1}$	It represents the i-th particle of the $(t+1)$-th generation.
$Food_k^t$	It denotes a particle randomly selected from N particles at generation t.
$Food_R^t$	It represents particles randomly selected from the first one-third of particles in the t-th generation, and as the iteration count increases, it increasingly favors selecting particles that were updated earlier.
$Food_m^{t+1}$	It is the particle that has been perturbed after the optimal particle or globally optimal particle has been updated in the mouth.
$Food_n^{t+1}$	It is the particle that has been perturbed after the optimal particle or globally optimal particle has been updated in the stomach.

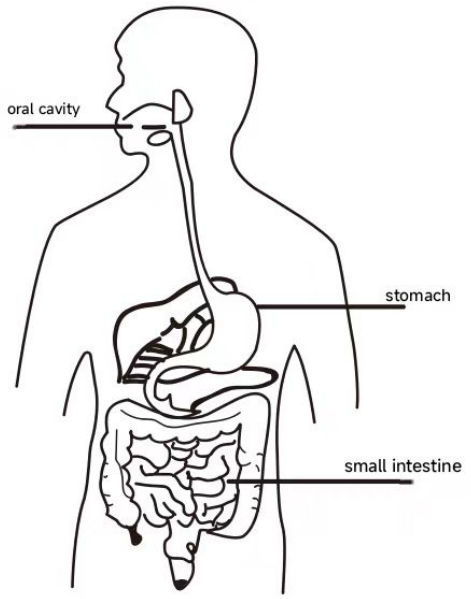

FIGURE 1. Food digestion site in the human body.

molars crush and grind the food as the tongue manipulates it. During this phase, saliva gradually mixes with the crushed particles. In the later stages, the food is thoroughly combined with saliva before passing through the pharynx and esophagus into the stomach.

In the stomach, physical digestion involves mechanical churning through peristalsis, contraction, and relaxation, while chemical digestion primarily consists of protein breakdown by pepsin. The upper end of the stomach connects to the esophagus, and its lower end connects to the duodenum. Food enters through the cardiac sphincter into the fundus, where the proximal stomach dilates to accommodate it—a process known as receptive relaxation. The food then moves toward the base of the stomach, mixing with gastric juices driven by peristaltic waves. This mechanical and chemical action further breaks down the food into chyme, which passes through the pyloric sphincter into the duodenum.

In the small intestine, physical digestion mainly involves segmental movements and food propulsion through peristaltic activity [40]. Chemical digestion involves various digestive enzymes working together to break down food.

2.2. **Mathematical Models and Algorithm.**

2.2.1. *Digestion in the oral cavity.* The digestion of food in the mouth is divided into two phases: physical and chemical. Physical digestion involves chewing and mixing food with the teeth and tongue, while chemical digestion involves the breakdown of food by enzymes—primarily salivary amylase—in the oral cavity. Within the oral cavity, the physical digestion of food primarily depends on mechanical forces, which are modeled as follows:

$$F1 = 2 * (-\arctan(iter * a/Max\_iter - a)) \tag{1}$$

$$F1\_d = 2 * F1 * rand - F1 \tag{2}$$

$F1$ decreases from 2 to 0 as the number of iterations increases, indicating that the force exerted by the mouth on the food gradually decreases over time. Max_iter represents the maximum number of iterations, while $iter$ denotes the current iteration. To ensure that the value of $F1$ remains between 0 and 1, we set a equal to the tangent of 1 and retain four decimal places, resulting in a value of $a = 1.5574$. $F1\_d$ refers to forces of varying magnitudes and directions, simulating the action of the teeth and tongue on the food. The variable $rand$ generates a random number between 0 and 1.

In the oral cavity, saliva mixes thoroughly with food, and the amylase in the saliva participates in the digestion of starch. This represents the chemical digestion process within the oral cavity. As food digestion progresses, the enzyme-catalyzed reaction initially accelerates and then decelerates; the concentration of the substrate also significantly influences the chemical digestion process. Taking these factors into account, the chemical digestion process of food in the oral cavity is modeled as follows:

$$Em^{(i)} = \begin{cases} 1 & if \quad r(i) > (D/2), r = randperm(D) \\ 0 & else \end{cases} \quad i = 1 \ldots D \tag{3}$$

$$V = (V_{\max} * S) \,/\, (K_m + S) \tag{4}$$

$$S = \sin(rand * \pi) \tag{5}$$

Em denotes the digestive enzyme, and its value is set according to Equation (3), where each dimension is randomly assigned a value of either 0 or 1, with exactly half of the dimensions set to 0 and the other half to 1. $randperm(D)$ indicates that the D dimensions are randomly permuted. Equation (4) represents the Michaelis–Menten equation, which describes the effect of substrate concentration on the enzymatic reaction rate [41]. $V_{\max}$ denotes the maximum enzyme reaction rate and is set to 2, as determined through extensive testing. V represents the rate of the enzymatic reaction. Equation (5) defines the substrate concentration S using a sinusoidal function, where π denotes the ratio of a circle's circumference to its diameter and $rand$ denotes a random number between 0 and 1. K_m is the Michaelis constant, a characteristic property of the enzyme that depends only on the enzyme's structure, the specific substrate, and the reaction conditions. It is independent of substrate concentration. The value of K_m was determined empirically and differs across the three digestive sites. In the oral cavity, K_m is set to 0.8. The particle update equation for the oral cavity is given below.

$$Food_i^{t+1} = Food_k^t + Phy1 + Chem1 \tag{6}$$

$$Phy1 = F1\_d * \left(C1 * Best\_p - Food_i^t\right) \tag{7}$$

$$Chem1 = C1 * Em * \left(Food_i^t - C2 * Food_R^t\right) * V \tag{8}$$

$$k = randi(N) \tag{9}$$

$$R = randi\left(ceil\left((N/3) * e^{-iter * b/Max\_iter}\right)\right) \tag{10}$$

Equation (6) represents the update equation for particles in the oral cavity. $Food_k^t$ denotes a particle randomly selected from the N particles at iteration t. $Phy1$ and $Chem1$ correspond to the update equations that simulate physical and chemical digestion of food

by particles in the oral cavity, respectively. $Best_p$ signifies the global optimal solution. The physical update process of a particle in the oral cavity is closely related to the global best position.

In Equation (8), R is an integer that decreases gradually as the number of iterations increases. $C1$ and $C2$ are random numbers that vary during the iterations, taking values in the intervals $(0, 2)$ and $(0, 1)$, respectively. The function *randi* returns a random integer, and *ceil* denotes the ceiling function, which rounds up to the nearest integer. The constant b, with a value of 1.5, is determined through function optimization.

Under ideal conditions, it is assumed that the quantity of food is equal across all three sites. The particle update order proceeds from the oral cavity to the stomach and then to the small intestine. At each of the first two sites, after each particle is updated, the best particle resulting from digestion at that site is identified and passed to the next site for further digestion.

2.2.2. *Digestion in the stomach.* The stomach lining contains a powerful muscular layer that facilitates the mixing of food with gastric juices through contractile movements known as peristalsis. This process ensures thorough contact between the food and digestive enzymes while further grinding the food into finer particles, constituting physical digestion in the stomach. Chemical digestion in the stomach is primarily mediated by enzymes, mainly pepsin. The mechanical forces acting on the food in the stomach are modeled as follows:

$$F2 = 2 * (1 - (iter/Max\_iter)) \tag{11}$$

$$F2\_d = 2 * F2 * rand - F2 \tag{12}$$

$F2$ decreases from 2 to 0 as the number of iterations increases. $F2\_d$ represents the force in various directions acting on the food in the stomach, with values in the interval $(-2, 2)$. In the stomach, the value of K_m is 0.9. The chemical digestion process of the particles in the stomach is modeled as follows:

$$Food_i^{t+1} = Food_m^{t+1} + Phy2 + Chem2 \tag{13}$$

$$Phy2 = F2\_d * \left(Food_i^t - C1 * Food_m^{t+1}\right) \tag{14}$$

$$Chem2 = C1 * Em * \left(Food_m^{t+1} - \ Mean\right) * V \tag{15}$$

$$Mean = \frac{1}{N}\left(\sum_{i=1}^{N/3} Food_i^{t+1} + \sum_{i=N/3}^{N} Food_i^t\right) \tag{16}$$

$$Food_m^{t+1} = \begin{cases} Food_m^{t+1} \\ Best\_p + \left(C1 * Best\_p - Food_m^{t+1}\right) \end{cases} \tag{17}$$

The selection condition of Equation (17) is $if \min\left(fitness_i^{t+1}\right) < Best\_p, i \in (1, N/3)$. That is, if the best solution among the first one-third of the particles after updating is better than the global best solution, the best particle from that subset is selected for updating; otherwise, the global best solution is perturbed, and the perturbed solution is used instead. The value of $Mean$ is computed using Equation (16).

2.2.3. *Digestion in the small intestine.* Physical digestion in the small intestine is primarily driven by peristaltic forces generated by the intestinal wall. Peristalsis refers to the process in which the small intestine propels food forward through rhythmic contractions and relaxations of its muscular layers. This mechanical movement thoroughly mixes the food with digestive juices, thereby increasing the contact area between the food and digestive enzymes and facilitating subsequent chemical digestion. Chemical digestion mainly

involves the action of digestive enzymes in the small intestine to break down food. The forces acting on the food in the small intestine are modeled as follows:

$$F3 = 2 * (-\arctan(iter * a/Max\_iter) + a_1) \tag{18}$$

$$F3\_d = 2 * F3 * rand - F3 \tag{19}$$

$F3$ decreases from 2 to 0 as the number of iterations increases, where a_1 (set to 1) adjusts the magnitude of the force. The constant a is set to 1.5574. $F3\_d$ is a random value uniformly distributed in $(-2, 2)$, representing the resultant force acting on the food in the small intestine. The variable $rand$ denotes a random number in the interval $(0, 1)$. Thus, the particle update equation in the small intestine is given by:

$$Food_i^{t+1} = Best\_p + Phy3 + Chem3 \tag{20}$$

$$Phy3 = F3\_d * \left(Food_i^t - C1 * Food_n^{t+1}\right) \tag{21}$$

$$Chem3 = C1 * Em * Levy(D) * V \tag{22}$$

$$Food_n^{t+1} = \begin{cases} Food_n^{t+1} \\ Best\_p + \left(C1 * Best\_p - Food_n^{t+1}\right) \end{cases} \tag{23}$$

The judgment condition for $Food_n^{t+1}$ is $if \min\left(fitness_i^{t+1}\right) < Best\_p, i \in (N/3, N * (2/3)))$, which is calculated from Equation (23). This condition implies that for particles updated in the stomach, if the best fitness value among the updated particles in this segment is better than the current global best solution, the corresponding particle is selected for further update. Otherwise, the global best particle is perturbed, and the perturbed version is used instead. Here, $Levy(D)$ denotes Lévy flight, computed according to Equation (24).

$$Levy(D) = 0.01 * \frac{\mu * \delta}{|v|^{\frac{1}{\beta}}} \tag{24}$$

$$\delta = \left(\frac{\Gamma(1+\beta) * sin(\frac{\beta * \pi}{2})}{\Gamma(\frac{1+\beta}{2}) * \beta * 2^{\frac{\beta-1}{2}}}\right)^{\frac{1}{\beta}} \tag{25}$$

β is a constant with a value of 1.5. μ and δ are random numbers between (0,1).

In summary, the pseudo-code for the food digestion algorithm is shown in Algorithm 1:

3. **Experimental Results and Analysis.** This section evaluates the algorithm's performance using the CEC2013 test set. We compare the Food Digestion Algorithm (FDA) with PSO [20], GA [26], DE [27], SCA [31], CSO [24], and AO [22]. By comparing the average values, standard deviations, and convergence curves of each algorithm on the 28 test functions, the advantages and disadvantages of each algorithm can be intuitively assessed.

3.1. **Parameter setting.** The experiments for FDA were conducted on a desktop computer with an Intel(R) Core(TM) i3-8100 CPU @ 3.60 GHz, 24 GB of RAM, and a 64-bit Windows 10 operating system. MATLAB R2018a was used to perform the experiments. The dimensionality was set to 50, the population size was 30, and each algorithm was independently run 20 times on each of the 28 test functions for 1000 iterations. Table 2 summarizes the parameter settings of each algorithm. Detailed parameter descriptions of the other algorithms can be found in [20, 22, 24, 26, 27, 31].

Algorithm 1 Food Digestion Algorithm

Input: Global optimum position $Best\_p$; Global optimal fitness value $Best\_f$;
Output: Population size N; Maximum number of iterations Max_iter; Dimension D; Lower boundary lb; Upper boundary ub;

Initialize the populations and calculate their fitness values;
Record the globally optimal solution $Best\_p$;
Initialize the parameters a, b, a_1, V_{max}, K_m;
while $iter < Max\_iter$ **do**
    Back up the initialized particle population and their fitness values;
    Calculate the values of $F1$, $F2$, $F3$ and R;
    Calculate the values of $C1$ and $C2$;
    for $i = 1 : N$ **do**
        Calculate the values of Em and S;
        if $i <= N/3$ **then**
            Calculate the values of $F1\_d$ and V;
            Update the positions of the particles according to Equation (6)) and calculate their fitness values;
            if $i == N/3$ **then**
                Find the minimum fitness value $fitness_m$;
                Update the particle according to Equation (17);
            end if
        end if
        if $i > N/3$ and $i <= 2 * N/3$ **then**
            Calculate the values of $F2\_d$, V, and $Mean$;
            Update the positions of the particles according to Equation (13)) and calculate their fitness values;
            if $i == 2 * N/3$ **then**
                Find the minimum fitness value $fitness_n$;
                Update the particle according to Equation (23);
            end if
        end if
        if $i > 2 * N/3$ **then**
            Calculate the values of $F3\_d$ and V;
            Update the positions of the particles according to Equation (20)) and calculate their fitness values;
        end if
    end for
    for $i = 1 : N$ **do**
        if Updated particle optimal fitness values > The historical optimal fitness value of the particle **then**
            Replace the updated particle's position and its fitness value with the historical best position and its fitness value of the particle;
        end if
    end for
    Backup the historical best position and its fitness value of the particle;
    Update the global optimal position and its fitness value;
    $iter = iter + 1$;
end while

TABLE 2. Parameters of the FDA algorithm.

Algorithm name	Parameter	value
FDA	a	1.5574
	b	1.5
	a_1	1
	V_{max}	2
	K_m	0.8, 0.9, 1
PSO	$Vmax$	6
	$Vmin$	-6
	c	2
GA	CR	0.9
	MR	0.4
DE	F	0.6
	Cr	0.4
SCA	a	2
CSO	$c1$	2
	MR	0.1
AO	$alpha$	0.1
	$delta$	0.1
	$omega$	0.005
	U	0.00565
	$r1$	10

3.2. **Complexity Analysis.** Complexity analysis primarily evaluates the computational resources and time required by an algorithm. Time complexity describes the relationship between the number of operations and the problem size, while space complexity refers to the amount of memory needed for data storage. As seen from the algorithm's pseudocode, the time complexity per iteration of FDA is $O(N * D)$. The space complexity required for storing the current population, historical best positions, and their fitness values is $O(2 * N * D) + O(2 * N)$. Since the space complexity of FDA is dominated by population storage, the overall space complexity per iteration is $O(N * D)$, where N represents the number of particles and D represents the dimensionality.

3.3. **Comparison with other algorithms.** In this section, we compare the mean and standard deviation of each algorithm on the test functions. The mean reflects the algorithm's optimization capability: a smaller mean indicates better performance. The standard deviation measures the algorithm's stability, with a smaller value indicating higher robustness. Table 3 and Table 4 summarize the experimental results. In these tables, values in bold indicate cases where other algorithms perform better than FDA. Table 3 provides the average values of the algorithm runs, and Table 4 lists the corresponding standard deviations. The last two rows in each table show the number of test functions where FDA outperforms or underperforms the other algorithms, respectively.

From Table 3, it can be observed that on the unimodal functions f1–f5, the optimality-seeking ability of FDA is slightly weaker than that of PSO but better than all other algorithms. This occurs because PSO consistently updates based on the best particle, enabling it to converge quickly and locate the optimum efficiently on unimodal functions, which have only one optimal value. In contrast, on multimodal and hybrid functions, FDA demonstrates stronger performance in finding the optimum. This advantage stems from the fact that each generation of particles in FDA is updated across three distinct

TABLE 3. Comparison results of the average values of each algorithm.

Function	PSO	GA	DE	SCA	CSO	AO	FDA
f1	-8.05E+02	1.14E+05	**-9.33E+02**	2.58E+04	-6.38E+02	8.31E+02	-9.09E+02
f2	**1.68E+07**	4.71E+09	4.02E+08	5.51E+08	4.02E+07	1.25E+08	3.21E+07
f3	**5.54E+09**	1.13E+21	3.25E+10	2.99E+11	1.70E+10	3.83E+10	1.03E+10
f4	**2.38E+04**	4.09E+06	9.07E+04	6.24E+04	**3.73E+04**	7.08E+04	4.63E+04
f5	-6.06E+02	5.94E+04	**-6.65E+02**	2.67E+03	-3.16E+02	-5.71E+01	-6.18E+02
f6	**-5.26E+02**	2.16E+04	**-5.66E+02**	1.41E+03	-4.31E+02	-2.97E+02	-5.10E+02
f7	-4.35E+02	3.10E+07	-4.28E+02	-3.02E+02	-4.37E+02	-3.26E+02	-4.45E+02
f8	-4.53E+02	-4.53E+02	-4.53E+02	-4.53E+02	-4.53E+02	-4.53E+02	-4.53E+02
f9	-3.58E+02	-3.48E+02	-3.49E+02	-3.49E+02	-3.57E+02	-3.57E+02	-3.59E+02
f10	-2.31E+02	1.87E+04	7.07E+02	3.20E+03	-3.28E+01	4.89E+02	-2.36E+02
f11	1.49E+02	1.58E+03	**-4.60E+01**	2.85E+02	1.80E+02	1.47E+02	5.08E+01
f12	2.91E+02	1.51E+03	**1.42E+02**	3.78E+02	2.42E+02	2.85E+02	2.41E+02
f13	3.89E+02	1.54E+03	**2.12E+02**	4.43E+02	3.89E+02	4.60E+02	3.65E+02
f14	5.40E+03	1.14E+04	7.21E+03	9.56E+03	5.45E+03	6.01E+03	4.72E+03
f15	**6.51E+03**	1.03E+04	1.01E+04	1.01E+04	**5.99E+03**	7.76E+03	6.96E+03
f16	1.36E+02	1.36E+02	1.36E+02	1.36E+02	**1.35E+02**	1.36E+02	1.36E+02
f17	**6.52E+02**	3.76E+03	**4.65E+02**	9.77E+02	**7.01E+02**	8.69E+02	7.26E+02
f18	**6.90E+02**	3.86E+03	**6.36E+02**	1.06E+03	**6.94E+02**	9.79E+02	7.99E+02
f19	3.97E+02	2.01E+07	**3.64E+02**	7.78E+04	4.14E+02	7.47E+02	3.74E+02
f20	4.16E+02	4.17E+02	4.16E+02	4.16E+02	4.16E+02	4.17E+02	4.16E+02
f21	**1.10E+03**	8.94E+03	1.17E+03	3.29E+03	1.43E+03	2.08E+03	1.11E+03
f22	8.04E+03	1.23E+04	8.42E+03	1.08E+04	8.66E+03	8.02E+03	6.58E+03
f23	8.79E+03	1.17E+04	1.10E+04	1.12E+04	8.53E+03	9.50E+03	8.47E+03
f24	9.37E+02	1.61E+03	**9.21E+02**	9.56E+02	9.64E+02	9.39E+02	9.36E+02
f25	1.05E+03	1.19E+03	**1.03E+03**	1.04E+03	1.09E+03	**1.02E+03**	1.04E+03
f26	1.09E+03	1.32E+03	1.06E+03	1.11E+03	1.07E+03	1.12E+03	9.71E+02
f27	2.29E+03	3.53E+03	2.36E+03	2.48E+03	2.37E+03	2.32E+03	2.29E+03
f28	4.07E+03	1.34E+04	**1.21E+03**	5.03E+03	4.04E+03	5.32E+03	3.49E+03
win	16	26	13	24	21	25	
lose	8	0	12	0	5	1	

sites, with interactions among particles from these sites enhancing both exploration and exploitation capabilities of the algorithm. Table 4 indicates that the stability of FDA is comparable to CSO and superior to other algorithms. Overall, FDA exhibits strong optimization performance and stability on most test functions and outperforms the other algorithms in comparison.

3.4. **Convergence analysis.** In this section, the ability of the algorithms to escape from local optima is evaluated by analyzing their convergence curves across 28 test functions. To mitigate the effects of randomness, each algorithm is executed 10 times on each function, and the average of these 10 runs is used for analysis. A data point is recorded every 50 generations for plotting purposes. Figure 2 shows the convergence curves of all the algorithms on selected functions.

The FDA algorithm performs particle updating across three digestive sites. During each iteration, the particle population is divided into three groups, each updated using a specific update equation. In the oral cavity, the current particle updates by following a randomly selected particle. This introduces uncertainty in the particle's position, enhances exploration, and increases population diversity. In the stomach, the current particle moves toward either the best particle from the previous site or a perturbed global best particle. This strategy helps balance exploration and exploitation, enabling the swarm to converge rapidly under the influence of a force that decreases over iterations. In the small intestine, particles follow the global best particle, fully leveraging their exploitation

TABLE 4. Comparison results of the standard deviation of each algorithm.

Function	PSO	GA	DE	SCA	CSO	AO	FDA
f1	6.83E+02	8.30E+04	6.71E+02	1.89E+04	**4.88E+02**	9.81E+02	6.54E+02
f2	**1.28E+07**	3.56E+09	3.02E+08	4.35E+08	3.09E+07	1.04E+08	2.46E+07
f3	**5.73E+09**	3.54E+21	2.44E+10	7.67E+11	1.37E+10	3.24E+10	9.91E+09
f4	**1.79E+04**	8.08E+06	6.60E+04	4.63E+04	**2.81E+04**	5.28E+04	3.36E+04
f5	**4.37E+02**	4.73E+04	4.78E+02	2.30E+03	**2.70E+02**	**2.15E+02**	4.44E+02
f6	3.82E+02	1.61E+04	4.07E+02	1.15E+03	**3.12E+02**	**2.25E+02**	3.70E+02
f7	**3.14E+02**	9.25E+07	**3.08E+02**	**2.50E+02**	**3.15E+02**	**2.64E+02**	3.21E+02
f8	**3.25E+02**	**3.25E+02**	3.26E+02	3.26E+02	**3.25E+02**	**3.25E+02**	3.26E+02
f9	2.58E+02	**2.51E+02**	**2.51E+02**	**2.51E+02**	**2.57E+02**	**2.57E+02**	2.58E+02
f10	1.99E+02	1.39E+04	5.50E+02	2.37E+03	**1.15E+02**	4.27E+02	1.76E+02
f11	1.28E+02	1.20E+03	**3.43E+01**	2.10E+02	1.61E+02	1.24E+02	6.67E+01
f12	2.36E+02	1.10E+03	**1.03E+02**	2.78E+02	1.98E+02	2.21E+02	1.87E+02
f13	2.89E+02	1.14E+03	**1.53E+02**	3.22E+02	2.93E+02	3.37E+02	2.71E+02
f14	3.96E+03	8.21E+03	5.20E+03	6.88E+03	3.99E+03	4.41E+03	3.43E+03
f15	**4.77E+03**	7.40E+03	7.24E+03	7.28E+03	**4.36E+03**	5.67E+03	5.09E+03
f16	9.77E+01	9.80E+01	9.79E+01	9.79E+01	**9.68E+01**	9.78E+01	9.76E+01
f17	**4.73E+02**	2.72E+03	**3.34E+02**	7.06E+02	**5.16E+02**	6.30E+02	5.28E+02
f18	**4.98E+02**	2.79E+03	**4.58E+02**	7.65E+02	**5.08E+02**	7.09E+02	5.79E+02
f19	3.42E+02	1.66E+07	**2.62E+02**	9.38E+04	3.01E+02	6.33E+02	2.69E+02
f20	2.99E+02	3.00E+02	2.99E+02	2.99E+02	2.99E+02	3.00E+02	2.99E+02
f21	8.07E+02	6.53E+03	9.41E+02	2.37E+03	1.09E+03	1.53E+03	8.07E+02
f22	5.83E+03	8.87E+03	6.06E+03	7.74E+03	6.29E+03	5.82E+03	4.80E+03
f23	6.40E+03	8.41E+03	7.92E+03	8.08E+03	**6.20E+03**	6.88E+03	6.21E+03
f24	6.74E+02	1.18E+03	**6.62E+02**	6.87E+02	6.94E+02	6.75E+02	6.73E+02
f25	7.56E+02	8.57E+02	**7.37E+02**	**7.50E+02**	7.87E+02	**7.35E+02**	7.51E+02
f26	7.84E+02	9.93E+02	7.68E+02	8.00E+02	7.77E+02	8.05E+02	7.03E+02
f27	1.65E+03	2.59E+03	1.70E+03	1.79E+03	1.71E+03	1.67E+03	1.65E+03
f28	3.50E+03	9.87E+03	8.69E+02	3.64E+03	3.53E+03	3.89E+03	3.38E+03
win	14	26	16	23	14	22	
lose	9	2	10	3	13	6	

capability. The use of Lévy flight to control the movement direction and step size assists the particles in escaping local optima.

Based on the update mechanisms of FDA and supported by the results in Table 3, Figure 2 reveals that the proposed algorithm exhibits slow convergence in the early stages. This occurs because the algorithm dedicates substantial effort to exploration initially. Extensive early-stage exploration helps increase particle diversity. As the number of iterations increases, the convergence rate gradually accelerates, ultimately leading to better solutions.

3.5. **Limitation of the FDA algorithm.** The FDA algorithm has certain limitations, in addition to its slow convergence during the early search phase as mentioned earlier. Our experiments revealed that the algorithm's performance was notably constrained when tested in lower-dimensional spaces. Table 5 presents the results of comparing the Food Digestion Algorithm (FDA) in 10 dimensions with six other classical algorithms. Algorithm performance is evaluated based on the average value (AVE) and the standard deviation (STD). The comparisons indicate the number of functions where FDA outperforms, matches, or is outperformed by the other algorithms. The remaining experimental settings are consistent with those described in Section 3.1. According to the results, FDA performs better than GA and SCA in terms of optimization capability but is inferior to the other algorithms. In terms of stability, FDA surpasses GA but is less stable than all

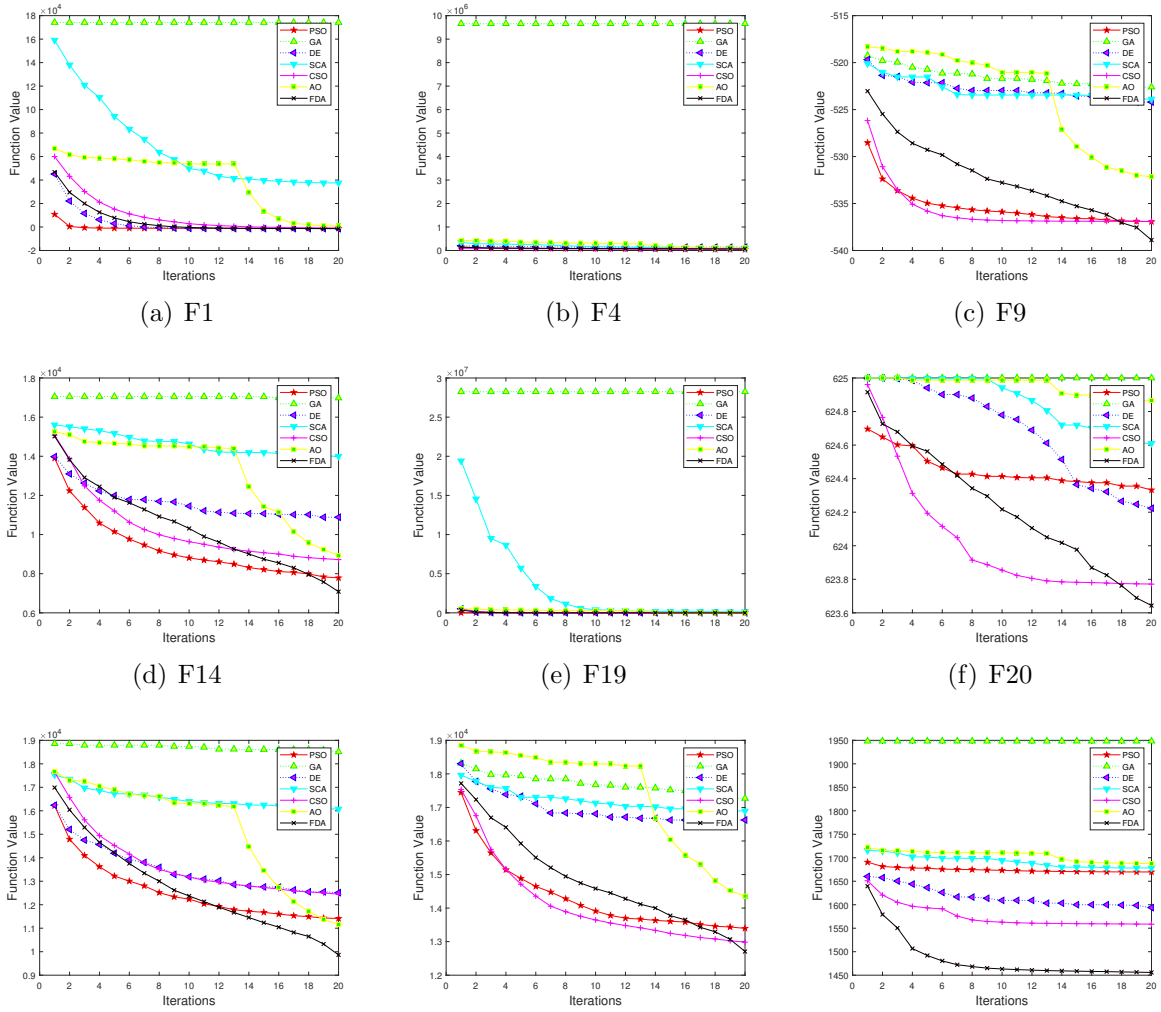

(a) F1 (b) F4 (c) F9

(d) F14 (e) F19 (f) F20

(g) F22 (h) F23 (i) F26

FIGURE 2. Convergence curve of the algorithms.

other algorithms. The instability observed in low-dimensional search spaces is identified as a contributing factor to the algorithm's suboptimal performance.

TABLE 5. Results of the run on ten dimensions.

	PSO	GA	DE	SCA	CSO	AO
AVE	10/2/16	27/1/0	7/0/21	19/0/9	8/1/19	12/1/15
STD	3/2/23	22/1/5	7/1/20	9/2/17	3/1/24	2/2/24

4. **Conclusion.** Inspired by the human digestive process, this paper proposes a novel meta-heuristic algorithm named the Food Digestion Algorithm (FDA). The algorithm divides the population into three update sites—oral cavity, stomach, and small intestine—to simulate different digestion stages. FDA was evaluated using 28 benchmark functions from the CEC2013 test suite and compared with six classical algorithms (PSO, GA, DE, SCA, CSO, and AO). Experimental results demonstrate that FDA achieves superior performance in both convergence speed and solution quality on most functions. Specifically, FDA exhibited better convergence than GA and SCA on all 28 functions, and outperformed PSO, DE, CSO, and AO on most functions. In terms of stability,

FDA surpassed all six comparison algorithms across all 28 test functions. However, a limitation was observed in low-dimensional search spaces, where FDA's stability requires further improvement in future work.

REFERENCES

[1] A. L. H. P. Shaik, M. K. Manoharan, A. K. Pani, R. R. Avala, and C.-M. Chen, "Gaussian mutation–spider monkey optimization (gm-smo) model for remote sensing scene classification," *Remote Sensing*, vol. 14, no. 24, p. 6279, 2022.

[2] K.-K. Tseng, R. Zhang, C.-M. Chen, and M. M. Hassan, "Dnetunet: a semi-supervised cnn of medical image segmentation for super-computing ai service," *The Journal of Supercomputing*, vol. 77, no. 4, pp. 3594–3615, 2021.

[3] V.-T. N. Trong-The Nguyen, Trinh Dong-Nguyen, "An optimizing pulse coupled neural network based on golden eagle optimizer for automatic image segmentation," *Journal of Information Hiding and Multimedia Signal Processing*, vol. 13, no. 3, pp. 155–164, 2022.

[4] T.-Y. Wu, H. Li, S. Kumari, and C.-M. Chen, "A spectral convolutional neural network model based on adaptive fick's law for hyperspectral image classification," *Computers, Materials & Continua*, vol. 79, no. 1, 2024.

[5] T.-Y. Wu, A. Shao, and J.-S. Pan, "Ctoa: Toward a chaotic-based tumbleweed optimization algorithm," *Mathematics*, vol. 11, no. 10, p. 2339, 2023.

[6] Z.-Y. Shao, J.-S. Pan, P. Hu, and S.-C. Chu, "Equilibrium optimizer of interswarm interactive learning strategy," *Enterprise Information Systems*, pp. 1–25, 2021.

[7] Z.-K. Zhang, P.-Q. Li, J.-J. Zeng, and X.-K. Liu, "Capacity optimization of hybrid energy storage system based on improved golden eagle optimization," *Journal of Network Intelligence*, vol. 7, no. 4, pp. 943–959, 2022.

[8] C.-M. Chen, S. Lv, J. Ning, and J. M.-T. Wu, "A genetic algorithm for the waitable time-varying multi-depot green vehicle routing problem," *Symmetry*, vol. 15, no. 1, p. 124, 2023.

[9] T.-Y. Wu, H. Li, and S.-C. Chu, "Cppe: An improved phasmatodea population evolution algorithm with chaotic maps," *Mathematics*, vol. 11, no. 9, p. 1977, 2023.

[10] J. Wu, M. Xu, F.-F. Liu, M. Huang, L. Ma, and Z.-M. Lu, "Solar wireless sensor network routing algorithm based on multi-objective particle swarm optimization," *Journal of Information Hiding and Multimedia Signal Processing*, vol. 12, no. 1, pp. 1–11, 2021.

[11] J.-Y. He, X.-Y. Hu, C.-C. Hu, M.-X. Wu, and M. Zhang, "Three-dimensional localization algorithm for wsn nodes based on hybrid rssi and dv-hop," *Journal of Network Intelligence*, vol. 7, no. 3, pp. 526–543, 2022.

[12] X. Li, S. Liu, S. Kumari, and C.-M. Chen, "Psap-wsn: A provably secure authentication protocol for 5g-based wireless sensor networks," *CMES-Computer Modeling in Engineering & Sciences*, vol. 135, no. 1, pp. 711–732, 2023.

[13] X. Kou and J. Feng, "Matching ontologies through compact monarch butterfly algorithm," *Journal of Network Intelligence*, vol. 5, no. 4, pp. 191–197, 2020.

[14] X. Xue, "A compact firefly algorithm for matching biomedical ontologies," *Knowledge and Information Systems*, vol. 62, no. 7, pp. 2855–2871, 2020.

[15] A. Kumari, V. Kumar, M. Y. Abbasi, S. Kumari, P. Chaudhary, and C.-M. Chen, "Csef: cloud-based secure and efficient framework for smart medical system using ecc," *IEEE Access*, vol. 8, pp. 107 838–107 852, 2020.

[16] T.-Y. Wu, Q. Meng, L. Yang, S. Kumari, and M. Pirouz, "Amassing the security: An enhanced authentication and key agreementprotocol for remote surgery in healthcare environment," *CMES-COMPUTER MODELING IN ENGINEERING & SCIENCES*, vol. 134, no. 1, pp. 317–341, 2023.

[17] L. Abualigah, A. Diabat, and Z. W. Geem, "A comprehensive survey of the harmony search algorithm in clustering applications," *Applied Sciences*, vol. 10, no. 11, p. 3827, 2020.

[18] S. Salcedo-Sanz, "Modern meta-heuristics based on nonlinear physics processes: A review of models and design procedures," *Physics Reports*, vol. 655, pp. 1–70, 2016.

[19] D. H. Wolpert and W. G. Macready, "No free lunch theorems for optimization," *IEEE Transactions on Evolutionary Computation*, vol. 1, no. 1, pp. 67–82, 1997.

[20] J. Kennedy and R. Eberhart, "Particle swarm optimization," in *Proceedings of ICNN'95-International Conference on Neural Networks*, vol. 4. IEEE, 1995, pp. 1942–1948.

[21] S. Mirjalili, S. M. Mirjalili, and A. Lewis, "Grey wolf optimizer," *Advances in Engineering Software*, vol. 69, pp. 46–61, 2014.

[22] L. Abualigah, D. Yousri, M. Abd Elaziz, A. A. Ewees, M. A. Al-Qaness, and A. H. Gandomi, "Aquila optimizer: a novel meta-heuristic optimization algorithm," *Computers & Industrial Engineering*, vol. 157, p. 107250, 2021.
[23] S. Mirjalili and A. Lewis, "The whale optimization algorithm," *Advances in Engineering Software*, vol. 95, pp. 51–67, 2016.
[24] S.-C. Chu, P.-W. Tsai, and J.-S. Pan, "Cat swarm optimization," in *Pacific Rim International Conference on Artificial Intelligence*. Springer, 2006, pp. 854–858.
[25] J.-S. Pan, L.-G. Zhang, R.-B. Wang, V. Snášel, and S.-C. Chu, "Gannet optimization algorithm: A new metaheuristic algorithm for solving engineering optimization problems," *Mathematics and Computers in Simulation*, vol. 202, pp. 343–373, 2022.
[26] J. H. Holland, "Genetic algorithms," *Scientific American*, vol. 267, no. 1, pp. 66–73, 1992.
[27] R. Storn and K. Price, "Differential evolution–a simple and efficient heuristic for global optimization over continuous spaces," *Journal of Global Optimization*, vol. 11, no. 4, pp. 341–359, 1997.
[28] E. Atashpaz-Gargari and C. Lucas, "Imperialist competitive algorithm: an algorithm for optimization inspired by imperialistic competition," in *2007 IEEE Congress on Evolutionary Computation*. IEEE, 2007, pp. 4661–4667.
[29] A. Faramarzi, M. Heidarinejad, B. Stephens, and S. Mirjalili, "Equilibrium optimizer: A novel optimization algorithm," *Knowledge-Based Systems*, vol. 191, p. 105190, 2020.
[30] E. Rashedi, H. Nezamabadi-Pour, and S. Saryazdi, "Gsa: a gravitational search algorithm," *Information Sciences*, vol. 179, no. 13, pp. 2232–2248, 2009.
[31] S. Mirjalili, "Sca: a sine cosine algorithm for solving optimization problems," *Knowledge-Based Systems*, vol. 96, pp. 120–133, 2016.
[32] J. J. Patricia and A. S. Dhamoon, "Physiology, digestion," *Europe PMc*, 2019.
[33] C. Hoebler, A. Karinthi, M.-F. Devaux, F. Guillon, D. Gallant, B. Bouchet, C. Melegari, and J.-L. Barry, "Physical and chemical transformations of cereal food during oral digestion in human subjects," *British Journal of Nutrition*, vol. 80, no. 5, pp. 429–436, 1998.
[34] W. C. Alvarez and A. Zimmermann, "Movements of the stomach," *American Journal of Physiology-Legacy Content*, vol. 84, no. 2, pp. 261–270, 1928.
[35] F. Kong and R. P. Singh, "A human gastric simulator (hgs) to study food digestion in human stomach," *Journal of Food Science*, vol. 75, no. 9, pp. E627–E635, 2010.
[36] M. Ferrua and R. Singh, "Modeling the fluid dynamics in a human stomach to gain insight of food digestion," *Journal of Food Science*, vol. 75, no. 7, pp. R151–R162, 2010.
[37] A. Guerra, L. Etienne-Mesmin, V. Livrelli, S. Denis, S. Blanquet-Diot, and M. Alric, "Relevance and challenges in modeling human gastric and small intestinal digestion," *Trends in Biotechnology*, vol. 30, no. 11, pp. 591–600, 2012.
[38] Q. Guo, A. Ye, N. Bellissimo, H. Singh, and D. Rousseau, "Modulating fat digestion through food structure design," *Progress in Lipid Research*, vol. 68, pp. 109–118, 2017.
[39] C. Hoebler, A. Karinthi, M.-F. Devaux, F. Guillon, D. Gallant, B. Bouchet, C. Melegari, and J.-L. Barry, "Physical and chemical transformations of cereal food during oral digestion in human subjects," *British Journal of Nutrition*, vol. 80, no. 5, pp. 429–436, 1998.
[40] L. R. Johnson and T. A. Gerwin, *Gastrointestinal physiology*. Mosby Elsevier Philadelphia, PA, 2007.
[41] L. Michaelis and M. L. Menten, "Die kinetik der invertinwirkung," *Biochem. z*, vol. 49, no. 333-369, p. 352, 1913.